Multitemporal Analysis of TRMM-Based Satellite Precipitation Products for Land Data Assimilation Applications

YUDONG TIAN

Goddard Earth Sciences and Technology Center, University of Maryland, Baltimore County, Baltimore, Maryland

CHRISTA D. PETERS-LIDARD AND BHASKAR J. CHOUDHURY

Hydrological Sciences Branch, NASA Goddard Space Flight Center, Greenbelt, Maryland

MATTHEW GARCIA

Goddard Earth Sciences and Technology Center, University of Maryland, Baltimore County, Baltimore, Maryland

ABSTRACT

In this study, the recent work of Gottschalck et al. and Ebert et al. is extended by assessing the suitability of two Tropical Rainfall Measuring Mission (TRMM)-based precipitation products for hydrological land data assimilation applications. The two products are NASA's gauge-corrected TRMM 3B42 Version 6 (3B42), and the satellite-only NOAA Climate Prediction Center (CPC) morphing technique (CMORPH). The two products were evaluated against ground-based rain gauge–only and gauge-corrected Doppler radar measurements. The analyses were performed at multiple time scales, ranging from annual to diurnal, for the period March 2003 through February 2006. The analyses show that at annual or seasonal time scales, TRMM 3B42 has much lower biases and RMS errors than CMORPH. CMORPH shows season-dependent biases, with overestimation in summer and underestimation in winter. This leads to 50% higher RMS errors in CMORPH's area-averaged daily precipitation than TRMM 3B42. At shorter time scales (5 days or less), CMORPH has slightly less uncertainty, and about 10%–20% higher probability of detection of rain events than TRMM 3B42. In addition, the satellite estimates detect more high-intensity events, causing a remarkable shift in precipitation spectrum. Summertime diurnal cycles in the United States are well captured by both products, although the 8-km CMORPH seems to capture more diurnal features than the 0.25° CMORPH or 3B42 products. CMORPH tends to overestimate the amplitude of the diurnal cycles, particularly in the central United States. Possible causes for the discrepancies between these products are discussed.

1. Introduction

The spatial and temporal structure of precipitation greatly impacts land surface hydrological fluxes and states (e.g., Fekete et al. 2003; Gottschalck et al. 2005). Accurate measurement of precipitation at fine space and time scales has been shown to improve our ability to simulate land surface hydrological processes and states, such as floods and droughts (Ogden and Julien 1993, 1994; Faures et al. 1995; Nykanen et al. 2001). In particular, previous results suggest that precipitation sampled at 3-h intervals or shorter significantly reduces uncertainties associated with flood prediction (Hossain and Anagnostou 2004; Nijssen and Lettenmaier 2004).

The anticipated Global Precipitation Measurement (GPM; Smith et al. 2007) mission is designed to provide high-resolution (~10 km) measurements of global precipitation from a deployed constellation of remote sensing satellites. GPM is expected to improve flood-hazard prediction capabilities from its high spatial- and temporal-resolution products, and from its reduced uncertainties in short-term precipitation accumulations (Steiner et al. 2003). For example, GPM will have 3-h average revisit time over 80% of the globe and provide these measurements in near–real time to end users.

Until recently, most operational precipitation products have climate-scale resolutions. Typically the horizontal spatial scales range from $2.5° \times 2.5°$ to $1° \times 1°$, and the time scales range from seasonal to monthly (e.g., Huffman et al. 1997, 2001; Gruber et al. 2000; Adler et al. 2001). Although these products are important for global climate-scale studies, they are insufficient for land surface hydrological research and applications, especially for regional or watershed-scale studies.

As prelude to GPM, the current operational Tropical Rainfall Measuring Mission (TRMM; Simpson et al. 1988; Kummerow et al. 2000), combined with other satellite platforms, has enabled a wide range of precipitation products. A few recent TRMM-based products are pathfinders for the planned GPM-based products; therefore, close examination of these interim products will provide insight and guidance to the upcoming GPM-era products.

Passive microwave (PMW)-based estimates of instantaneous precipitation are more accurate than infrared (IR)-based algorithms (e.g., Adler et al. 2001), because of the stronger relationship between the microwave radiance and the precipitation. The GPM-era satellites will extend the PMW-based measurements to the next decade, and with further improvement of the algorithms, we expect they will have significant impact on our study of climate change, global water cycles, as well as short-term processes such as flash floods.

Operational satellite-based remote sensing of precipitation with passive microwaves started with the Defense Meteorological Satellite Program (DMSP) Special Sensor Microwave Imager (SSM/I; Hollinger et al. 1990) platforms in the 1990s. The addition of TRMM platform launched in 1997 provided additional coverage with its TRMM Microwave Imager (TMI) sensor. By merging TMI, SSM/I, and other Earth Observing System (EOS)-era sensors, such as the Advanced Microwave Sounding Unit (AMSU) and the Advanced Microwave Scanning Radiometer for EOS (AMSR-E), and incorporating IR data from geostationary satellites in one way or another, various groups have recently produced global precipitation products with high spatial and temporal resolutions. The resolution of these products is approaching that of the future GPM products.

Among these products are TRMM 3B42RT and 3B42 Version 6 (3B42) produced at the National Aeronautics and Space Administration (NASA) Goddard Space Flight Center (GSFC) from the TRMM Multisatellite Precipitation Analysis (TMPA; Huffman et al. 2007), and the Climate Prediction Center (CPC) morphing technique (CMORPH) produced at the National Oceanic and Atmospheric Administration's (NOAA)

CPC (Joyce et al. 2004). These multisensor products rely heavily on the PMW measurements from TRMM and other satellites, with high space and time resolution (3 h and 0.25°), near-real-time availability and near-global coverage. CMORPH has an even higher-resolution version, with a space and time resolution of 8 km and 30 min, respectively. These level 3 products are well formatted with their data on regular geographical grids. These features make them appealing in land data assimilation applications (e.g., Gottschalck et al. 2005).

Because of the rather recent availability of these products, there have not been many efforts to evaluate and intercompare each product. Gottschalck et al. (2005) evaluated the real-time version of TRMM 3B42 (3B42RT) among a collection of model, satellite, and merged precipitation products over the contiguous United States (CONUS), at a resolution of 0.25° and at daily to seasonal time scales. They found that 3B42RT did not compare favorably with other precipitation products, especially in terms of bias, and somewhat in terms of daily correlations, although it outperformed several products with respect to temporal correlation across the U.S. Great Plains during the summer. Ebert et al. (2007) compared 12 satellite- and model-based precipitation products, including two TRMM-based estimates, 3B42RT and CMORPH, over CONUS, Australia, and Europe. Their results showed the satellite-based products, as a group, performed best in summer. Over CONUS, satellite products had higher correlations with surface gauge measurements in the eastern half of the country as compared to the western half.

In this study we extend the work by Gottschalck et al. (2005) and Ebert et al. (2007) in three aspects. First, we introduce 3B42, which is gauge corrected, instead of 3B42RT, for our analysis. This will illustrate the impact of gauge correction on the satellite estimates, and such results will shed light for both algorithm developers and data end users. We also extend their study period from 1 yr (2002) to 3 yr. Second, we will first revisit the CONUS-scale results, and then focus on a smaller-scale domain, namely, the southeast United States (SE-US), where TRMM coverage is maximized and the effects of topography are minimized to examine fine spatial features enabled by these high-resolution datasets. Such finescale studies are more useful for applications at typical watershed scales, and the pixel-level details connect more directly to the algorithms deriving the estimates from satellite swaths. Finally, the existing studies have not looked into subdaily time scales enabled by the high temporal resolution of these products, which have 3 h or higher time resolutions. We aim to fill this gap in our work.

In particular, we will examine the diurnal variability

of precipitation over CONUS (e.g., Dai et al. 1999) as observed by the satellites. Recently, Yang and Smith (2006) studied the diurnal variability of precipitation in TRMM's level 2 datasets with a $5° \times 5°$ resolution. Such a spatial resolution is not enough to resolve fine features at a subcontinental scale such as CONUS. Janowiak et al. (2005) analyzed the diurnal cycle of CMORPH data at a 3-hourly time scale on the global scale and half-hourly for regional analysis at 0.25° resolution, and compared with surface radar data for a single season over the United States. In this work, we address the unresolved issue of how the features in the diurnal cycles in CMORPH compare with other datasets, such as TRMM 3B42, or compare with CMORPH's own higher-resolution version (8 km, 30 min).

In the present study we evaluate and intercompare TRMM 3B42 and CMORPH, with their native resolution whenever possible. We study the datasets from the perspective of end users for hydrological land data assimilation studies. We focus our study over CONUS, especially the SE-US. Scientifically, the SE-US region was chosen to maximize the coverage of the TMI, while minimizing the impacts of topography on the gauge- and radar-based estimates. Further, this area is largely free of ice, snow cover, and desert, which will complicate the PMW-based retrievals over the land surface (Grody 1991; Ferraro et al. 1998). The variety of climate regimes in the SE-US region, including tropical/subtropical and maritime/continental, are also helpful for testing these products. We describe our datasets and methods in detail in section 2. Results will be presented in section 3, with analysis at multiple time scales from annual/seasonal to hourly, including the error distribution as a function of time scale. Conclusions are given in section 4.

2. Data and methodology

We focus our studies on two high-resolution precipitation products: the GSFC TRMM 3B42 Version 6 product and the CMORPH product suite. Another GSFC TRMM product with the same space–time resolution as 3B42, 3B42RT (real time) product, will not be presented here, because existing studies have examined it extensively, and in some sense the information in 3B42RT is a subset of 3B42. Our own analyses, as well as recent discussions with the project scientists (G. J. Huffman and R. F. Adler 2006, personal communication) indicated that the inclusion of monthly gauge-based bias corrections in 3B42 greatly reduces errors relative to the 3B42RT product analyzed by Gottschalck et al. (2005) and Ebert et al. (2007). Moreover,

it is important to note that each 3B42RT field is processed with the then-current (experimental) algorithm, whereas 3B42 is uniformly processed with a frozen version (G. J. Huffman 2007, personal communication) making it more suitable for a multiyear evaluation.

A simplified version of the data flow for both the GSFC TRMM and the CMORPH products is shown in Fig. 1. Both CMORPH and 3B42 derive their precipitation estimates primarily from PMW measurements. These PMW measurements are from a combination of satellites, including TRMM, DMSP, NOAA, and the more recent EOS platforms, to obtain maximum coverage and enhanced temporal sampling. In 3B42, PMW sensors were intercalibrated to TRMM's combined PR and TMI retrievals, while CMORPH used TMI and SSM/I as calibration reference, with TMI having the highest precedence whenever available.

Both datasets use IR data from geostationary satellites as well, to deal with PMW coverage gaps. However, they use the IR data differently. CMORPH uses the high-resolution IR imagery to infer the motion of precipitation patterns between PMW scans, and use this advection information to obtain a smooth "morphing" of PMW rain patterns between PMW snapshots, thus obtaining rain estimates between PMW swaths (Joyce et al. 2004). The 3B42 product, on the other hand, uses PMW-calibrated IR precipitation estimates directly, to fill the PMW coverage gaps.

Another difference between 3B42 and CMORPH is that 3B42 incorporates surface gauge measurement information, while CMORPH is purely satellite derived. The 3B42 product, after merging PMW- and IR-based estimates, the individual 3B42 3-hourly precipitation values are then scaled to sum to a combination of monthly 3B42 and gauge analysis, which is TRMM product 3B43. The gauge analysis uses the Global Precipitation Climatology Center (GPCC; Rudolf et al. 1994) monthly gauge dataset, which was in turn derived from measurements by about 6700 stations over the globe.

The CMORPH suite has two high-resolution versions, one with the same space and time resolution as 3B42, and the other with much higher resolution, 8 km and 30 min. We studied both products at their native resolutions. We denote the 0.25° version as CMOR0.25, and the 8-km version as CMOR8km when we use both simultaneously; otherwise we use CMORPH to refer to the 0.25°, 3-h version, which matches the 3B42 resolution.

CMORPH products coverage starts from December 2002, while 3B42 goes back to 1998. We selected a maximum overlapping time span of three complete
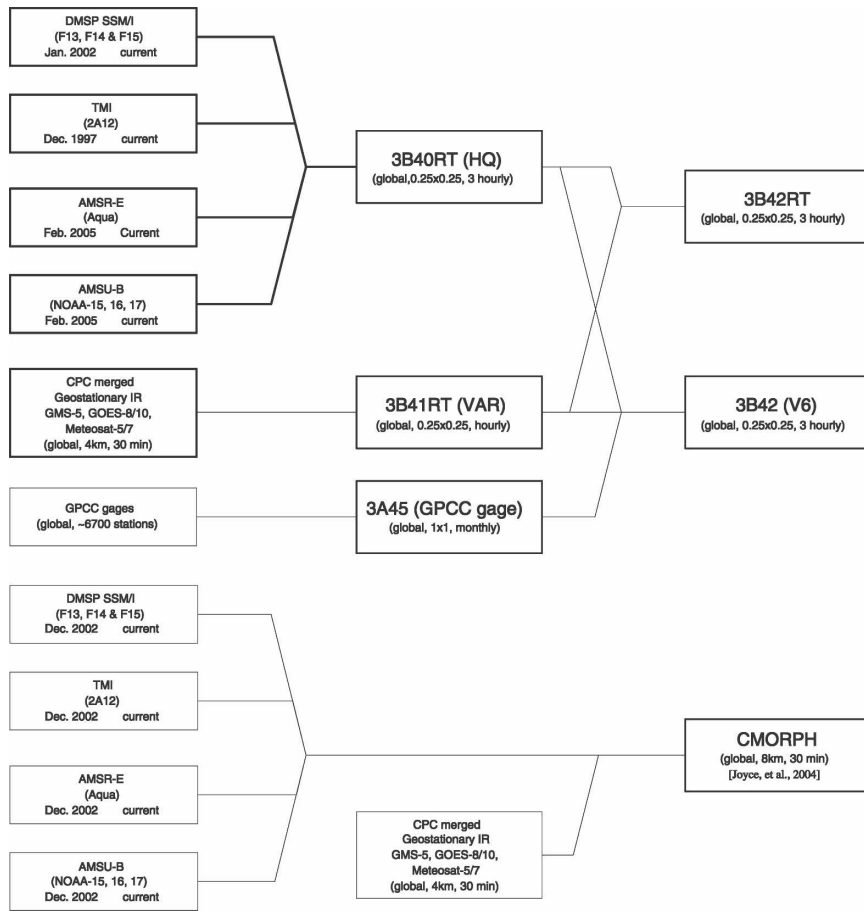
Fig. 1. Genealogy of the TRMM-era precipitation products to be studied, 3B42 and CMORPH. A sister product of 3B42, 3B42RT, is also shown.

years for CMORPH and 3B42, from March 2003 to February 2006, as our study period.

Similar to Gottschalck et al. (2005) we used two ground-based precipitation estimates as reference data to evaluate the satellite products. One is the National Centers for Environmental Prediction (NCEP) stage IV data (Lin and Mitchell 2005), which are primarily based on the Next-Generation Weather Radar (NEXRAD) measurements, optimally merged with hourly gauge reports based on the multisensor precipitation estimator (MPE; Seo 1998) algorithm, and with manual quality control. This hourly dataset has a spatial resolution of approximately 4 km.

The other reference dataset is the NCEP CPC near-real-time daily precipitation analysis (Higgins et al. 2000), denoted here as "Higgins," which is a daily, 0.25° product. This dataset is derived from the daily reports of 6000–7000 CPC Cooperative rain gauges over United States, with some quality control measures including duplicate station checks, buddy checks, and standard deviation checks against climatology. In addi-

tion, Higgins estimates use ground-based radar estimates to eliminate spurious zeros reported by a small portion of the gauges (Higgins et al. 2000).

It is worth noting that the gauge information contained in stage IV and Higgins are from two different networks. The hourly gauge reports in the NCEP stage IV estimates are from the Hydrometeorological Automated Data System (HADS), with 5000–6000 reports over the United States. The Higgins analysis does not use the data from HADS network, though it may incorporate it in future versions. Gottschalck et al. (2005) have shown that stage IV and Higgins data are much better correlated than other model- or satellite-based products, suggesting that both are valuable reference products.

We used both stage IV and Higgins data for evaluations at daily or longer time scales, and intercompare them whenever possible. For subdaily time scales, only the hourly stage IV is available for comparison with 3B42 and CMORPH, as Higgins's time resolution is daily. There are mismatches between time step bound-
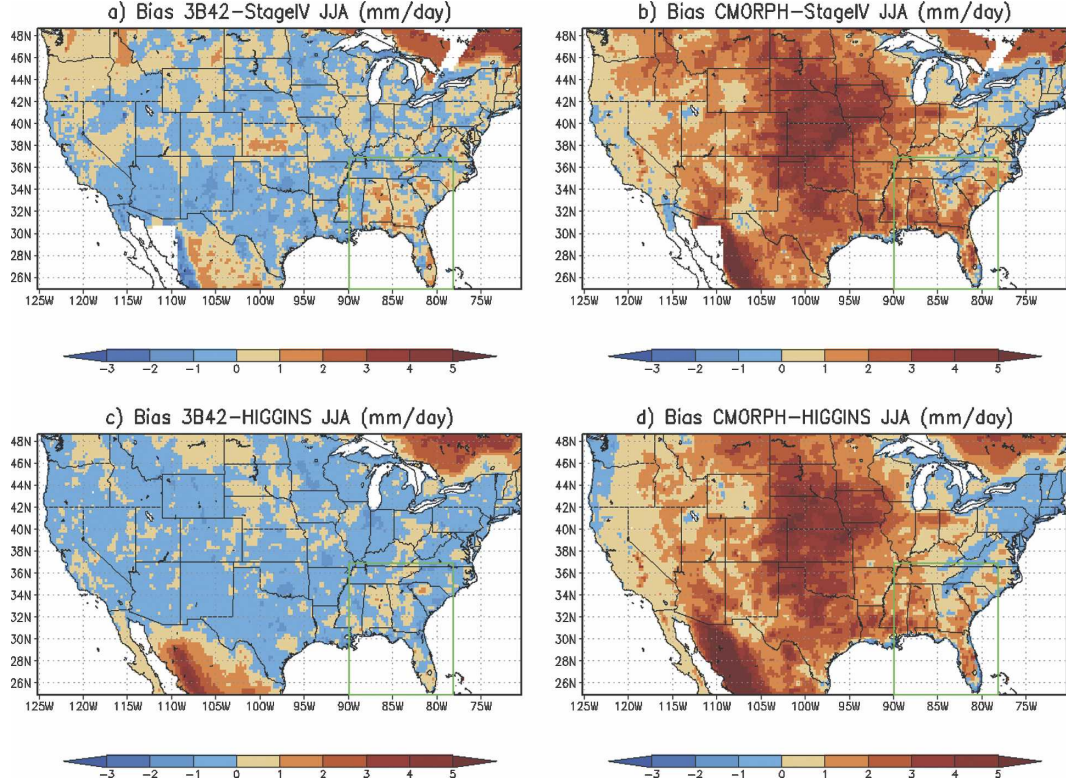
FIG. 2. Mean difference (mm day^{-1}) in summer (JJA) precipitation between (a) 3B42 and stage IV; (b) CMORPH and stage IV; (c) 3B42 and Higgins; and (d) CMORPH and Higgins, over the 3-yr study period. The green box shown in each panel indicates the SE-US area in our study.

aries and spatial grids in the four datasets. For example, Higgins's daily accumulation is centered at 1200 UTC, and its 0.25° grid has a half gridbox shift from 3B42 and CMORPH's 0.25° grid. We ensure temporal and spatial matchups by interpolating or aggregating them onto a common grid, and this step is critical for correct analysis of these datasets. There is a negligible amount (<1%) of missing data in each product in our study period over most part of CONUS, especially over the SE-US region. Stage IV is missing about 90% of the data in the northwest corner of CONUS, roughly between 43°–50°N and 115°–125°W, however.

3. Results

a. Climatology studies over CONUS

We start with the evaluation of 3B42 and CMORPH for 3-yr seasonal accumulations at 0.25° spatial resolution over CONUS. Seasonal accumulations were calculated and compared with both stage IV and Higgins. Figures 2 and 3 show the mean difference of daily precipitation over CONUS between the two satellite products and two ground-based estimates, for summer [June–August (JJA)] and winter [December–February

(DJF)] seasons, respectively, which may be compared to Figs. 8 and 14 in Gottschalck et al. (2005). In summer (Fig. 2), 3B42 has relatively small biases in the range of −1 and 1 mm day^{-1} over most areas of CONUS. CMORPH, on the other hand, has large overestimates over the central United States, and slight underestimates over the northeast United States. The performance of CMORPH is consistent with the performance of satellite-only products shown in Gottschalck et al., and the benefits of the monthly bias correction in 3B42 are evident when comparing the results presented here to the original "Huffman" (3B42RT) results shown in Fig. 8 of Gottschalck et al. In the SE-US region (the green box in each panel), 3B42 shows random patches of positive and negative biases, while CMORPH is dominated by fairly large overestimates.

In winter (Fig. 3), 3B42 still has relatively small biases over most of CONUS, but shows large underestimates over the west coast when compared to Higgins estimates. CMORPH suffers similar underestimation problems there, with slightly larger amplitude. In addition, CMORPH exhibits fairly large underestimates over the northeast United States, larger than that in summer (Fig. 2). Comparing to Fig. 14 in Gottschalck et
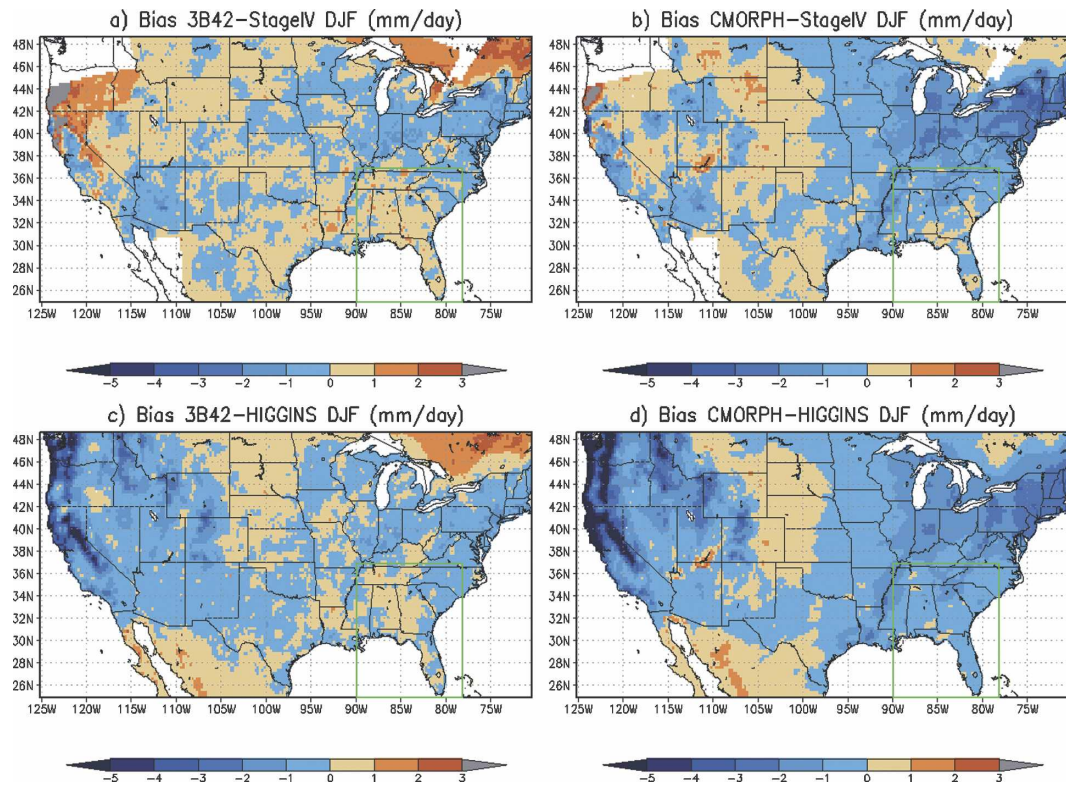
FIG. 3. As in Fig. 2, but for winter (DJF).

al. (2005), the 3B42 results suggest that the bias corrections have not solved the 3B42RT problems in the western coast range and Sierras—although the degree to which the Higgins product properly represents topographic gradients would require further investigation (e.g., Briggs and Cogley 1996). The underestimation problem is not as evident in the West Coast when stage IV is used as the reference. This is due to the large amount of missing data in stage IV in this area, and the results are not reliable here. Over the SE-US region, 3B42 does not show a consistent trend, but CMORPH has a tendency to underestimate ($\sim$1 mm day^{-1}) there (e.g., Fig. 3d).

We also produce the time correlation of daily precipitation between satellite and ground-based products, for summer (JJA; Fig. 4) and winter (DJF; Fig. 5), respectively. These figures may also be compared to Figs. 5 and 9 in Gottschalck et al. (2005), and similar to the results presented therein. Figure 4 shows that there is a clear west–east gradient in correlation in summer, for both 3B42 and CMORPH, with the eastern half of the country having higher correlation than the western half. In addition, CMORPH has slightly higher correlation than 3B42 in the eastern half. Systematic low correlations can be seen over the Sierra Nevada region. In the SE-US region, the inland areas tend to have higher

correlation than the coastal areas, including the entire state of Florida.

The winter season (Fig. 5) sees an even more dramatic correlation pattern. High correlation between the satellite and ground-based products is concentrated in the southeast quarter of the United States, with a sharp gradient separating it from other areas. The northwest quarter has very low correlation values, and so does the southwest, except for the coastal areas. In addition, CMORPH has slightly higher correlation and larger spatial extent than 3B42 in the southeast quarter. In the SE-US region, the correlation is comparatively high ($>$0.6) for both 3B42 and CMORPH, although there is some suggestion of lower correlations along the southern Appalachians.

We speculate the low correlation areas shown in Fig. 5, mostly in higher latitudes or over mountainous areas, may be attributed to two factors: 1) the deficiency of IR-based algorithms in detecting precipitation from stratiform cloud systems, especially in winter (e.g., Vicente et al. 1998), and 2) the interference of ice and snow cover over land surfaces to PMW-based retrievals (e.g., Grody 1991; Ferraro et al. 1998). It remains to be determined quantitatively the impact of these factors, but it is clear that in extratropical areas and in cold seasons, satellite-based precipitation retrievals are still
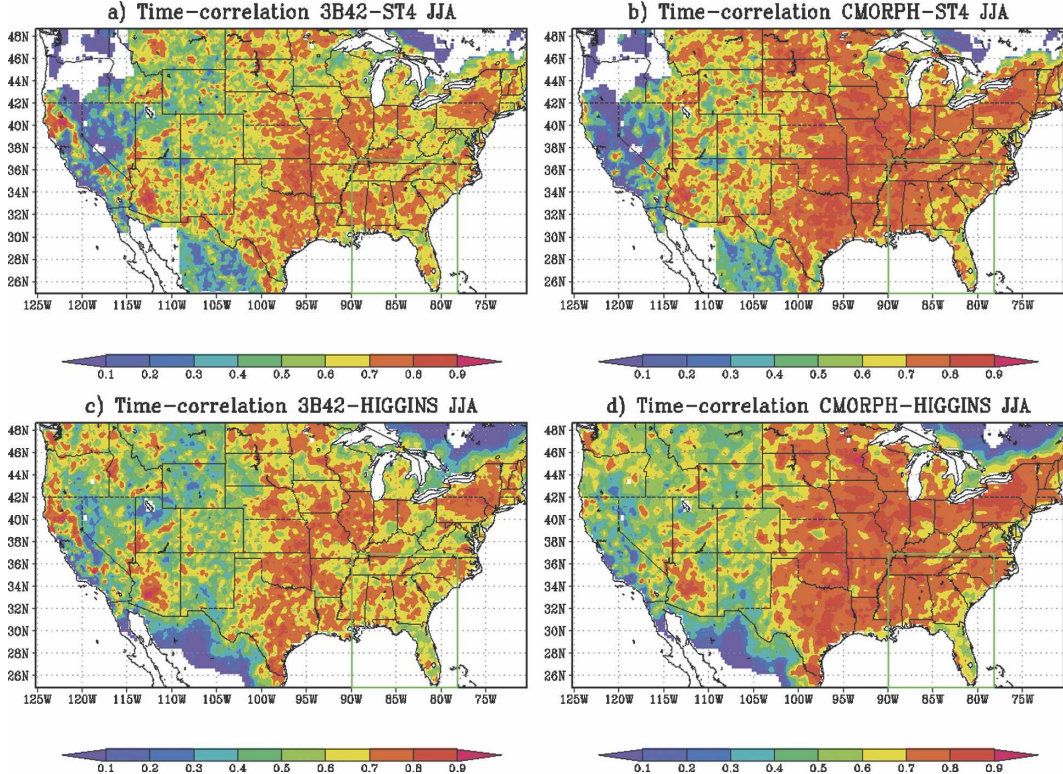
FIG. 4. Time correlation of daily precipitation for summer (JJA) between (a) 3B42 and stage IV; (b) CMORPH and stage IV; (c) 3B42 and Higgins; and (d) CMORPH and Higgins, over the 3-yr study period. The green box shown in each panel indicates the SE-US area in our study.

a challenging task. On the other hand, our focused study area, SE-US, is largely free of these issues, and thus provides us with a setting to study the performance of these products under favorable conditions and to establish a baseline for the current state of the science.

b. Focused studies over SE-US

Figures 6 and 7 show scatterplots between the satellite- and ground-based products for summer and winter total precipitation, respectively, over each $0.25° \times 0.25°$ grid point in the SE-US region. Overall, 3B42 shows less scattering than CMORPH against either stage IV or Higgins, for both seasons (Figs. 6a,c and 7a,c. Especially in summer (Fig. 6), 3B42 shows very high correlation with the ground-based datasets, especially Higgins. CMORPH suffers from season-dependent biases, with overestimates in summer and underestimates in winter (Figs. 6b,d and 7b,d), a similar tendency as over CONUS shown in last section. It is clear that the GPCC-based monthly amplitude-adjustment algorithm used in 3B42 greatly helps it to reduce the bias in long-term aggregations, such as the seasonal and annual time scales in our case. We suspect the season dependency of

CMORPH's biases may be related to the performance of scattering-based PMW algorithms over different precipitation regimes, with better retrieval over strong, convective precipitation in summer, in particular.

Figure 8 shows a few spatial statistical measures as functions of time, computed from the daily precipitation in each dataset over SE-US. Each dataset was aggregated to the daily time scale, to match that of the Higgins dataset. Bias, RMSE, spatial correlation, and probability of detection (POD; see Ebert et al. 2007 for a nice explanation) were computed daily for the entire 3-yr period (1 March 2003 through 28 February 2006). The daily time series of these statistics are shown in Fig. 8 after applying a 31-day moving average to remove high-frequency fluctuations for clarity.

There are strong seasonal variations in these statistics for both 3B42 and CMORPH. Both 3B42 and CMORPH show higher RMSE, correlation, and POD in summer than winter. For example, in the summer of 2004, the daily spatial correlation for both CMORPH and 3B42 is in the range of 0.6–0.75, while in the winter it drops to 0.3 (Fig. 8c). In addition, CMORPH shows high positive-bias episodes in summer and smaller negative bias in winter, while 3B42 does not have a
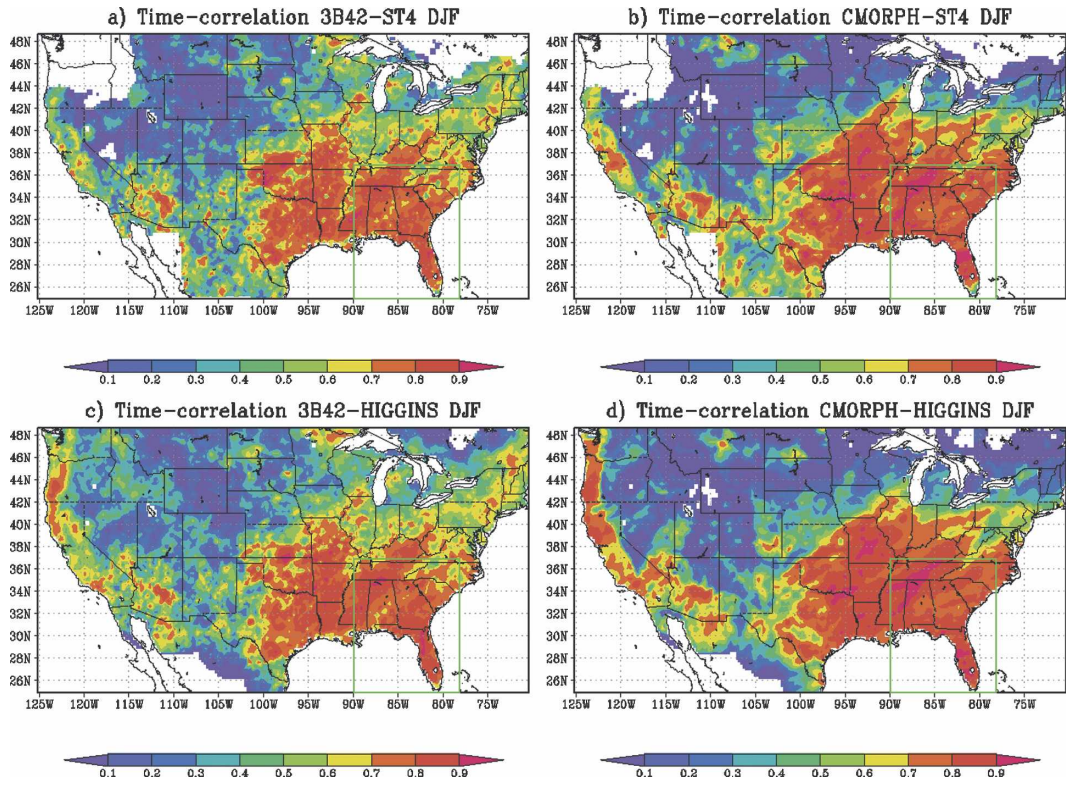
FIG. 5. As in Fig. 4, but for winter (DJF).

strong seasonal variation in bias estimates (Fig. 8a). This is consistent with the seasonal time-scale studies shown in the previous section, and in Figs. 6 and 7.

However, the correlation and POD results in Figs. 8c and 8d suggest that CMORPH is better than 3B42 at detecting daily time-scale precipitation events. Moreover, in winter, the daily RMSE of 3B42 is slightly higher than CMORPH, suggesting that the monthly bias-removal approach in 3B42 does not help the overall performance if the precipitation events are not correctly detected in the first place. It seems the morphing technique used in CMORPH helps this product catch more events on the daily time scale. As shown in Fig. 8c, CMORPH has slightly higher correlation than 3B42 with either stage IV or Higgins. For example, in the first summer, CMORPH has about 15% higher correlation with ground-based data than 3B42.

For POD, CMORPH also performs slightly better than 3B42, especially in summer (Fig. 8d), with similar seasonal variations. CMORPH consistently has about 10% higher POD than 3B42. For instance, at the beginning of July 2004, CMORPH has a POD of nearly 90% against stage IV, while 3B42 has about 80%.

To help data producers diagnose the POD behaviors in particular, we show in Figs. 9 and 10, respectively, the spatial distribution of POD, and its accompanying false alarm rate (FAR; e.g., Ebert et al. 2007), computed from daily precipitation data over the 3-yr period. Indeed, over SE-US, CMORPH has higher POD values, especially over most inland areas, than 3B42. On the other hand, both products show problematic, low PODs along the coastlines. This might be related to the known issue of joining the two different classes of algorithms for overland and overocean PMW retrievals (Adler et al. 1993). Along the northern border of the SE-US domain, 3B42 has particularly low PODs, possibly due to the decreased amount of convective precipitations at higher latitudes.

The FAR plots (Fig. 10) show that when averaged over the 3 yr, 3B42 and CMORPH have similar FAR amplitudes in SE-US; albeit there are differences in the spatial patterns. In particular, both 3B42 and CMORPH show isolated higher FAR patches in the inland areas, and it seems they are related to the presence of water bodies. Along the Florida coastlines, 3B42 shows remarkably higher FARs, indicating some inconsistencies with coastal pixel retrievals. These issues deserve further study elsewhere.

Figure 11 shows (a) the intensity distribution of the averaged number of annual precipitating days and (b) annual averaged precipitation accumulation. The former can be regarded as the probability distribution
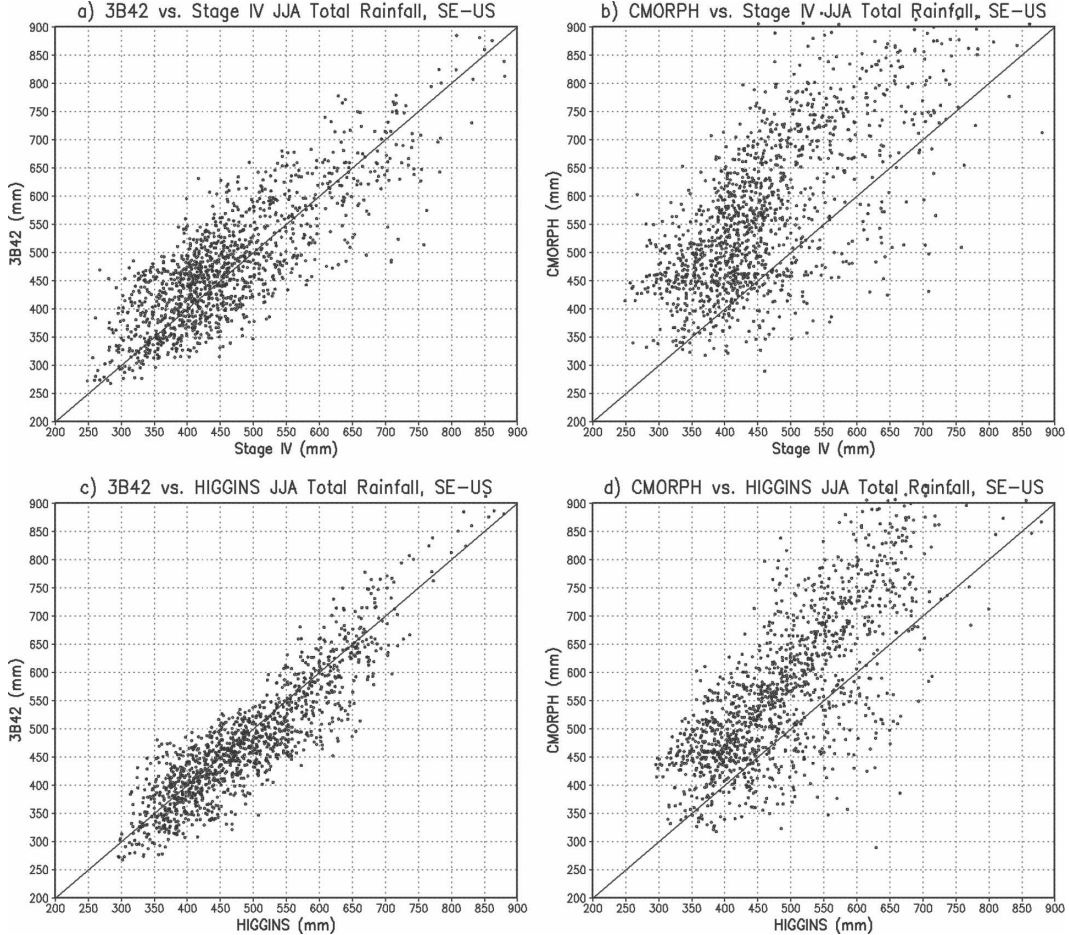
Fig. 6. Scatterplots of 3-yr average summer precipitation (mm) at each grid point over SE-US between (a) 3B42 and stage IV; (b) CMORPH and stage IV; (c) 3B42 and Higgins; and (d) CMORPH and Higgins.

function (PDF) of precipitating days, and the latter as the PDF, or "spectrum" of total precipitation. Figure 11a shows, for precipitation intensity in the range of 1 to ~25 mm day^{-1}, Higgins sees the most precipitating days, followed by the other reference dataset, stage IV. The two satellite datasets both have less precipitating days than the reference datasets, with 3B42 having the least. This partially explains the difference in POD pattern shown in Fig. 9. Over ~25 mm day^{-1}, the trend is reversed and there are more precipitating days in the satellite datasets. In other words, the satellite-based estimates detected more strong precipitation events than the ground measurements. Consequently, this caused a "spectrum" shift (Fig. 11b), with the ground measurements having a peak around 22 mm day^{-1} and the satellite estimates having most precipitation around 35 mm day^{-1}. At the light rain range (0.1–1 mm day^{-1}), CMORPH has spurious, large fluctuations in the number of precipitating days (Fig. 11a), but they do not contribute much to the total precipitation (Fig. 11b).

We speculate that the causes for such differences between ground-based and satellite estimates come from two sources. On one hand, the satellite PMW-based algorithms are good at detecting strong, convective precipitation events, but tend to miss shallow and warm rains. That will likely shift the "spectrum" to the higher-intensity end. The bias correction in 3B42 will also boost the amplitude of detected events to compensate for the would-be contribution from missed events. On the other hand, one of the ground-based datasets, Higgins, is spatially interpolated from point measurements, and strong events tend to spill to adjacent grid boxes, leading to more events but with reduced intensities. Stage IV also uses surface gauge measurements to adjust its estimates, probably having a similar flattening effect as Higgins. These factors will shift the ground-based estimates toward the low-intensity end of the spectrum.

The "spectrum" difference shown in Fig. 11 has remarkable implications for land surface data assimila-
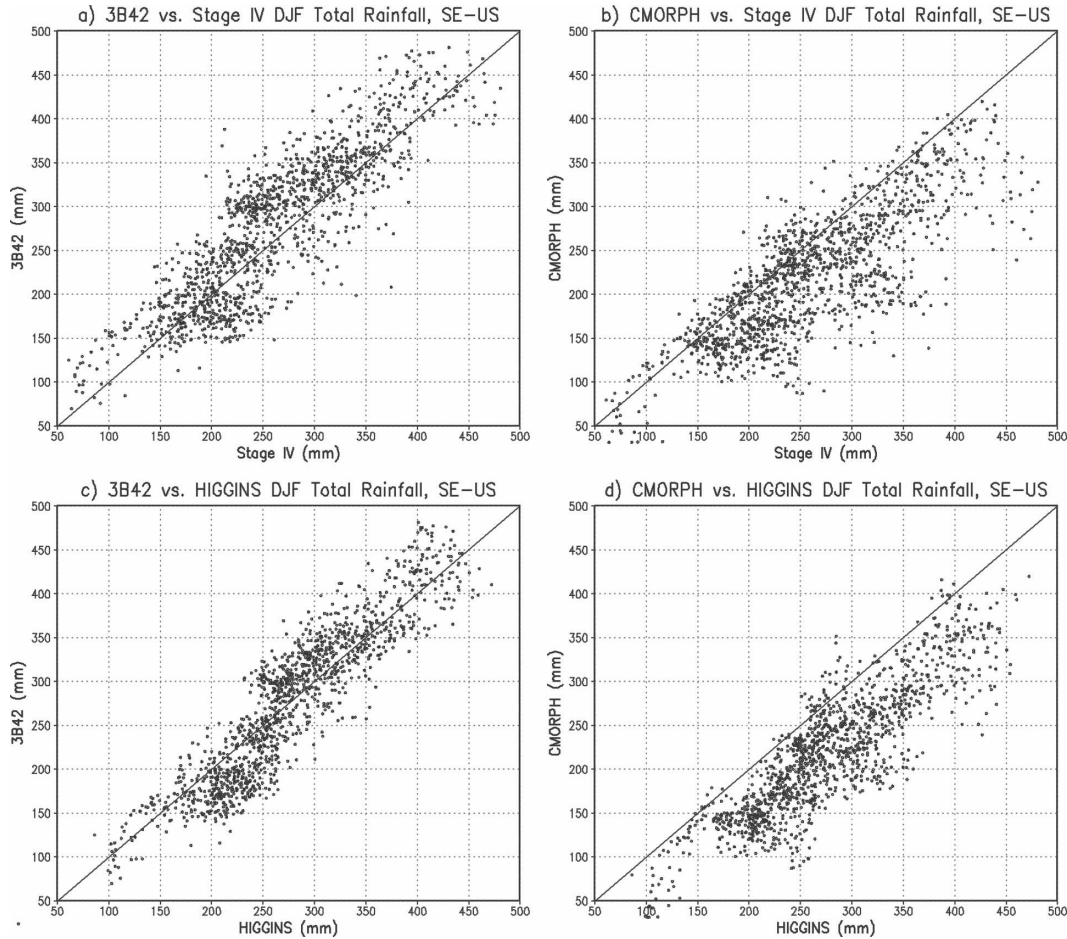
FIG. 7. As in Fig. 6, but for winter (DJF).

tion, especially for surface runoff and flood modeling. Because the land surface runoff processes are strongly nonlinear (Fekete et al. 2003), the shift in the distribution of precipitation intensity will cause significant differences in runoff production, partly because strong rainfall events are much more efficient in generating surface runoff. Therefore, we expect the satellite products will overestimate surface runoff as compared to the ground-based counterparts and will tend to produce more flood warnings if applied in flood modeling applications, even when the data are less biased, such as 3B42.

c. Diurnal cycles over CONUS

The high temporal and spatial resolutions of 3B42 and CMORPH enable us to study the diurnal cycles in precipitation in detail. Figures 12 and 13 show the results of the diurnal variation analysis for summer (JJA), for 3B42, CMOR0.25, CMOR8km, and stage IV. Figure 12 displays the amplitude of the diurnal harmonics

computed by discrete Fourier analysis of the 3-yr climatology data for the respective seasons and products. Figure 13 shows the actual diurnal climatology time series sampled at eight locations over the CONUS domain, including part of the North American Monsoon Experiment (NAME) region. The estimates were analyzed at their native spatial and temporal resolutions:

3B42: 0.25°, 3 h;
CMOR0.25: 0.25°, 3 h;
CMOR8km: 8 km, 0.5 h;
Stage IV: 4 km, 1 h.

In summer, there are strong diurnal signals in precipitation over CONUS in all four estimates (Fig. 12). These signals are mainly concentrated in four regions: the SE-US, the Great Plains, off the Carolina coast, and the NAME region. The diurnal cycles in SE-US and NAME are generally stronger than the other two regions in all the datasets. Overall, the two versions of CMORPH (CMOR0.25 and CMOR8km) are consistent with each other as shown in Fig. 12. Both
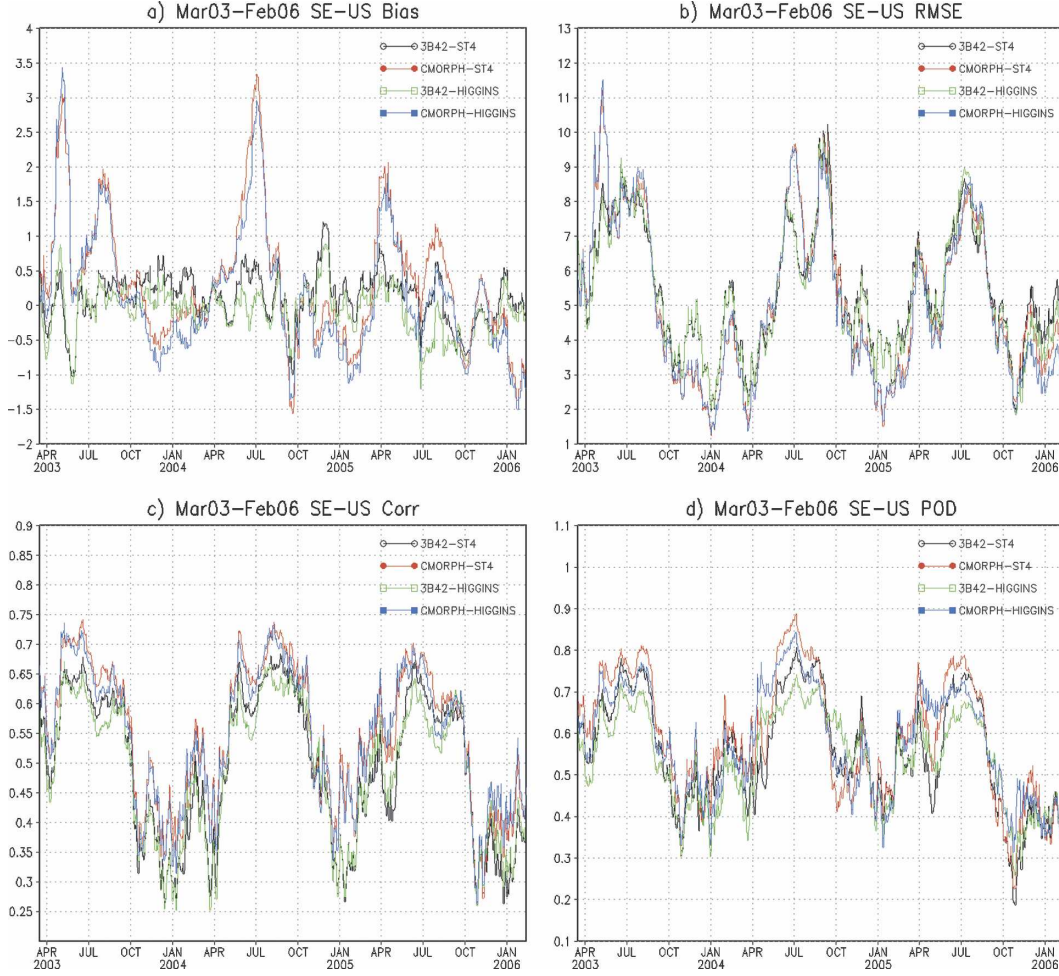
FIG. 8. Daily time series of spatial statistical and skill measures (bias, RMSE, spatial correlation, and POD) between the satellite-based and the ground-based products, over SE-US, for the 3-yr study period from March 2003 through February 2006. A 31-day moving average was performed on each time series to smooth the curves. In computing POD, a threshold of 1 mm day^{-1} was used.

CMOR0.25 and CMOR8km tend to exhibit stronger diurnal signals in summer than 3B42 and stage IV, especially in the Great Plains and the NAME region, where both CMORPH products' diurnal cycles are about twice as strong as the other two datasets. CMORPH also shows the geographical coverage of diurnal variations is much larger in these two regions. For instance, CMORPH shows diurnal cycles over most of the Great Plains, whereas 3B42 and stage IV display limited coverage.

The strong summer diurnal cycles in precipitation can also be seen from the climatology time series, shown in Fig. 13. Here eight grid points were sampled from the four regions shown in Fig. 12, for 3B42, CMOR0.25, CMOR8km, and stage IV. Higgins data are also shown at each location for reference, without diurnal variations due to their daily time resolution.

The diurnal cycles from all four products are well reproduced, with closely aligned phases (e.g., Orlando, Florida). The higher amplitudes from CMORPH over the Great Plains and the NAME region shown in Fig. 12 also manifest themselves at Culiacan, Mexico, and Haigler, Nebraska, in Fig. 13.

The phases of the diurnal cycles from the four datasets are fairly close to each other; no systematic differences can be seen. The phase differences in diurnal variations at different geographical locations are well reproduced in every dataset. The five sites examined over SE-US [Jacksonville, Tampa, Orlando, Tallahassee, and Kennedy Space Center (KSC), Florida] have the same phase, with precipitation peaking around 3 p.m. local solar time (LST). In the NAME region, precipitation reaches a maximum between 6 and 9 p.m. The site at Haigler, Nebraska, shows a similar phase.
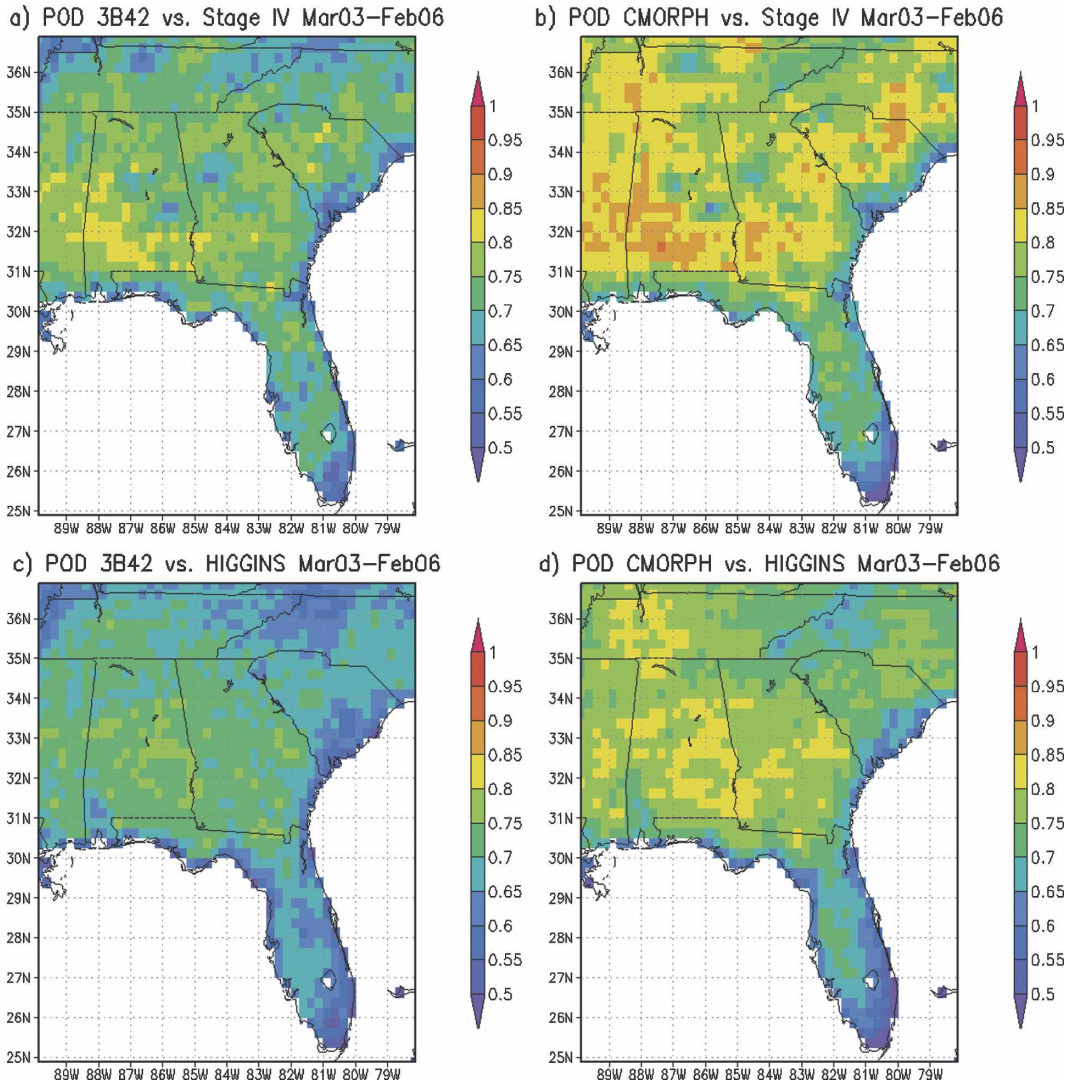
FIG. 9. Spatial distribution of daily precipitation POD for (a) 3B42 vs stage IV; (b) CMORPH vs stage IV; (c) 3B42 vs Higgins; and (d) CMORPH vs Higgins, over the 3-yr study period. A threshold of 1 mm day^{-1} is used to define a precipitating day.

It is also notable that the phase of the diurnal cycle in the ocean off the Carolina coast is quite different from that over land: the peak of precipitation occurs in the morning. Yang and Smith (2006) reviewed the possible mechanisms for the different diurnal variability over ocean and over land. The features seen here are overall consistent with other studies with PMW-based measurements (Imaoka and Spencer 2000; Janowiak et al. 2005), but the geographical location and phase of the diurnal variability are much better defined in our analysis due to the use of the high-resolution data.

In contrast, no strong, systematic diurnal variations in precipitation are seen in other seasons (not shown). For example, in winter, the overall amplitude of the diurnal cycle is much smaller than that shown in Fig. 12,

and there are no consistent locations of diurnal variations. Both 3B42 and stage IV show some weak structures on the west coast of CONUS, but CMORPH products do not support that feature. All four products also exhibit weak diurnal signals with scattered patterns over east and southeast CONUS, without much agreement among each other, except for between CMOR0.25 and CMOR8km. Tallahassee, Florida, is an exception, where the four datasets consistently show a weak diurnal cycle. The diurnal amplitude there is about 30%–50% of its summer counterpart.

d. Error distribution with time scales

In the previous sections we examined the precipitation products at a few separate time scales, from sea-
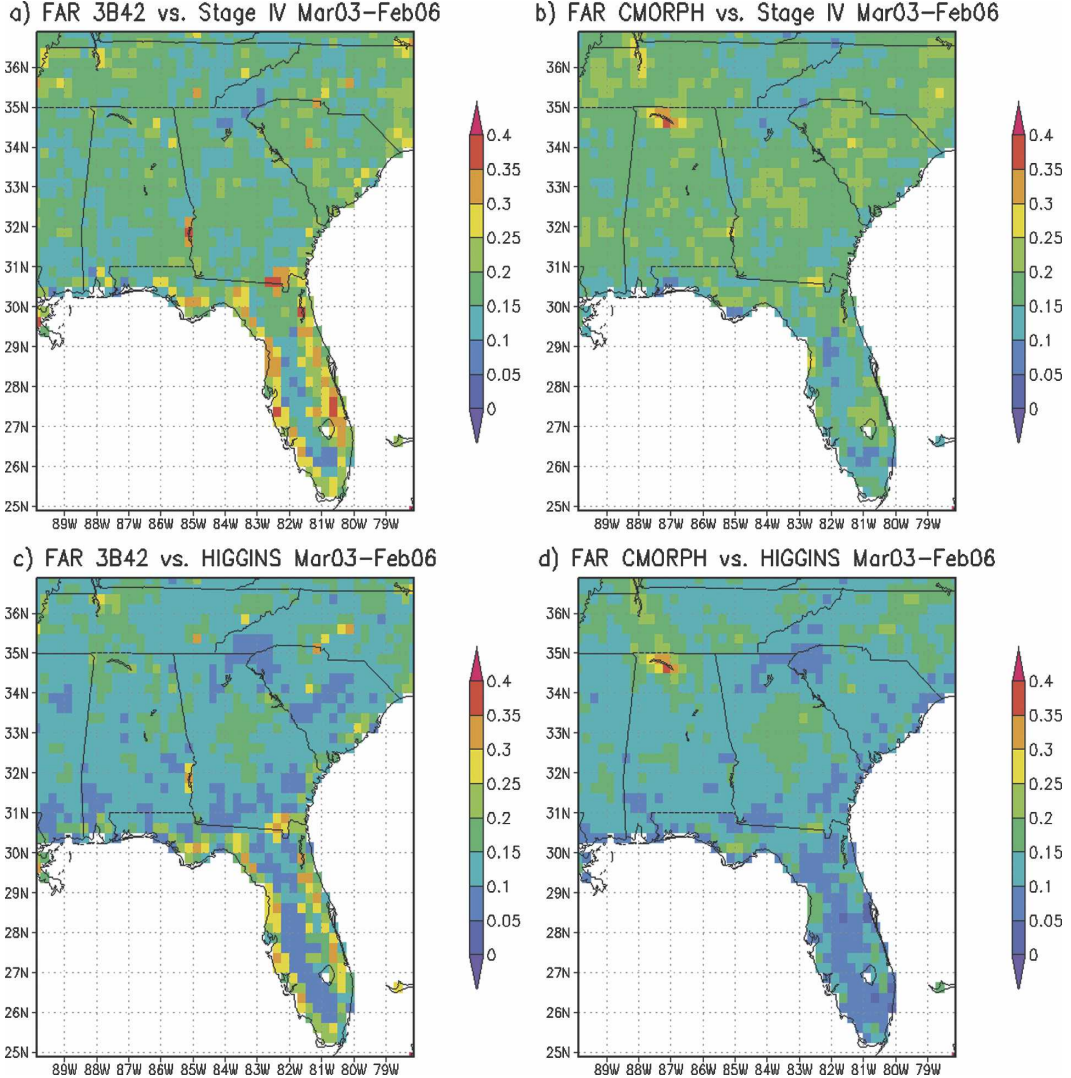
FIG. 10. As in Fig. 9, except for FAR.

sonal down to diurnal. To obtain a bigger picture of the error characteristics across time scales, we computed the errors in the satellite-based products as a function of time scales, ranging from 1 to 30 days. The results are shown in Figs. 14 and 15. We first computed running averages for each precipitation dataset with averaging time scales from 1 to 30 days. We then computed the RMSE of 3B42 and CMORPH against stage IV and Higgins at each time scale, and averaged the RMSE values at each time scale over the 3-yr period, producing the results shown in Fig. 14. It shows the uncertainties in each satellite dataset as a function of the time scale. We can see that, when the time scale is larger than 5 days, CMORPH has more uncertainty than 3B42 when compared either to stage IV or Higgins. However, for the short time scales of less than 5 days, the

RMSE values are very close between 3B42 and CMORPH, with CMORPH's RMSE slightly smaller than 3B42. This indicates that, though the gauge information in 3B42 did help with errors at long time scales, it did not improve the short-time-scale errors, since the scaling could not create or eliminate rain events. It seems CMORPH's "morphing" technique improves the inference of rain events, thus providing slightly less uncertainty at the event time scale (1–5 days).

We also computed the errors at each averaging time scale on each day and produced the errors of each product as a function of time and time scale. Figure 15 shows these errors for (a) 3B42 and (b) CMORPH compared with stage IV data.

Figure 15 shows some interesting features. First, most large errors at long time scales originated from short-
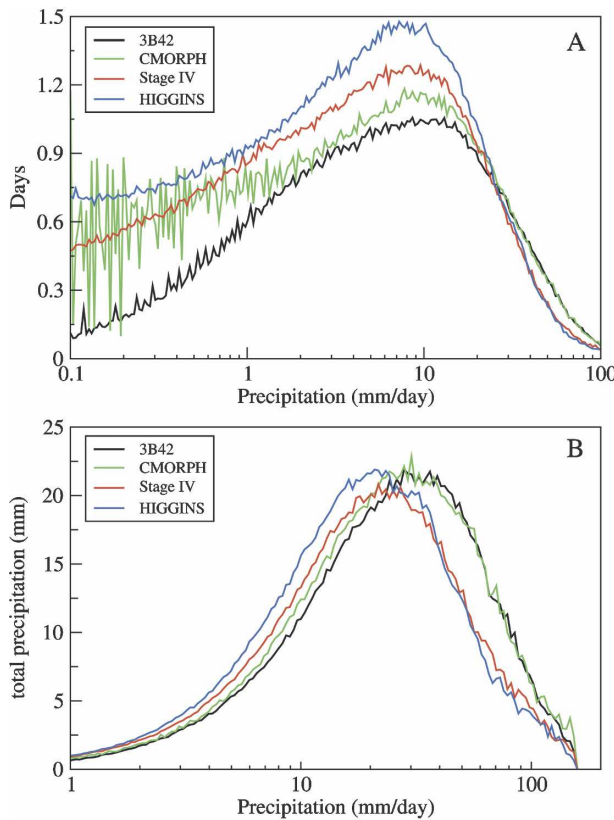
FIG. 11. Precipitation intensity distribution of (a) average number of precipitating days per grid per year, and (b) average total precipitation per grid per year, for the four datasets over SE-US, for the 3-yr study period. The precipitation intensity range shown on the abscissa of each figure is discretized into 200 bins in a logarithmic scale for the statistics. There are about 1300 grid points over land in the SE-US domain.

time-scale errors, as short as the minimum, 1-day time scale. This is particularly evident for CMORPH data. For example, a large positive bias in the summer of 2004 can be traced back to contributions from a few individual events around July 2004. The biases in such short-time-scale events accumulate all the way to the monthly time scale, contaminating the long-time-scale averages for months before and after these short-lived episodes. Similar features can be seen for the spring and summer seasons of 2003 and 2006 for CMORPH, and in early summer 2003 and midwinter 2004 for 3B42, though with smaller amplitudes. Figure 15 also highlights the intermittent and skewed nature of precipitation, with fewer but stronger events dominating the accumulation and errors over a fairly long time scale. This is consistent with the shifted spectra shown in Fig. 11.

Second, the errors at longer time scales in 3B42 are much smaller than in CMORPH, and their extent in the time domain is also more limited. There is a clear ten-dency of error reduction when the time scale is larger than about 10 days in 3B42, so that the errors from short-lived events at daily time scales do not influence the long-time-scale errors as much as for CMORPH. For example, in 3B42, the strong positive biases in the winter of 2003 at daily time scales only led to slight overestimates at time scales longer than 15 days. In contrast, almost all the short-lived events in CMORPH produced pronounced errors at longer time scales. Similar features can be observed when 3B42 and CMORPH are compared to Higgins (not shown). We conclude that the reduced errors at longer time scales in 3B42 can be attributed to the amplitude adjustment to its 3-hourly estimates using the monthly gauge-based 3B43 data.

4. Conclusions

Precipitation measurements from TRMM and GPM have great potential for hydrologic studies and land data assimilation applications. We evaluated and compared two recent satellite-based precipitation products, TRMM 3B42 and CMORPH, against two ground-based products, stage IV and Higgins. The two satellite-based products feature high spatial and temporal resolutions and are primarily based on passive microwave measurements of presumably high accuracy. We investigated the quality of 3B42 and CMORPH on diurnal to annual time scales over CONUS, and especially over the southeast United States (SE-US). We also studied the error distribution from short to long time scales. Based on our investigation, we conclude the following:

1) When aggregated to annual or seasonal time scales, 3B42 shows much lower bias and higher correlation with either stage IV or Higgins data. CMORPH has lower correlation values with a positive bias annually, resulting from a large positive bias in summer and a small negative bias in winter (Figs. 2–7).
2) On daily time scales, however, CMORPH correlates slightly better with the ground-based measurements than 3B42 and with significantly higher POD (Figs. 8–10). However, CMORPH suffers large positive bias in summer and negative bias in winter during the 3-yr study period. Both products correlate to ground-based measurements better in summer (0.60–0.75) than in winter (0.30) (Fig. 8).
3) Both 3B42 and CMORPH successfully capture the diurnal cycles in the summer precipitation over CONUS. The occurrence of strong diurnal variability is confined to four observed regions: SE-US, the Great Plains, off the Carolina coast, and the NAME region. The amplitude of diurnal variations from
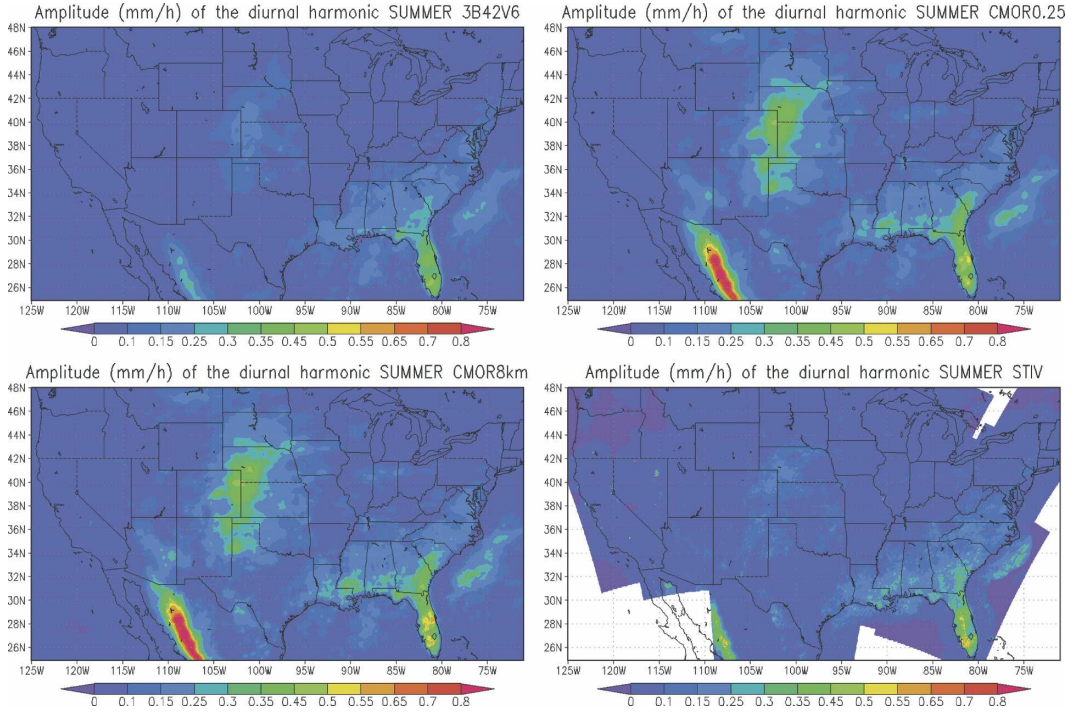
FIG. 12. Amplitude (mm h^{-1}) of the diurnal cycle computed from the 3-yr climatology of 3B42, CMOR0.25, CMOR8km, and stage IV, respectively, over CONUS for summer season (JJA). The time resolutions of the climatology data are the same as the real-time data, i.e., 3 h, 3 h, 30 min, and 1 h for 3B42, CMOR0.25, CMOR8km, and stage IV, respectively. Part of the NAME region is also shown.

3B42 is closer to that of the ground-based radar observations. CMORPH demonstrated much stronger diurnal cycles in the Great Plains and the NAME region (Fig. 12). The high spatial resolutions of these datasets enabled us to better define the geographical locations of strong diurnal cycles than previous studies (e.g., Dai et al. 1999).

4) Incorporation of rain gauge information in 3B42 greatly reduces its bias on longer time scales, and improves spatial correlation over SE-US when aggregated over seasonal and annual time scales. However, at daily time scales, 3B42 does not show an advantage over CMORPH in RMSE, spatial correlation, or POD (Fig. 8). Instead, CMORPH performed slightly better in these measures at short time scales.

5) Satellite-based estimates show more intense events than ground-based ones (Fig. 11), causing a systematic shift in precipitation "spectrum." Even if the satellite data were unbiased in total accumulation, such intensity shift will have significant impact on surface runoff applications.

It is not particularly surprising to see that 3B42 more closely corresponds to the ground-based estimates at seasonal time scales, because 3B42 incorporates ground-based monthly gauge data to adjust the amplitude of precipitation. However, we want to point out that for such an approach to be more successful, better performance in event detection is critical. Otherwise, and as most clearly demonstrated by examining the PDF of precipitation, the magnitude of the detected events will be incorrectly increased or reduced at the expense of the missed events, skewing the intensity distribution.

The latency in the availability of 3B42 resulting from the monthly bias correction also limits its usefulness in real-time applications, such as flood monitoring. However, both the CMORPH results presented here and the original "Huffman" product results presented in Gottschalck et al. (2005) show that intensity-, location-, and topography-dependent biases remain an issue for TRMM-based multisensor precipitation products. Based on the body of work now available, we propose that the data producers consider adopting a moving window of 30-day accumulations for bias correction processing, instead of the current calendar-month-based one. This would eliminate the latency and enable a bias-corrected product as timely as 3B42RT or CMORPH.
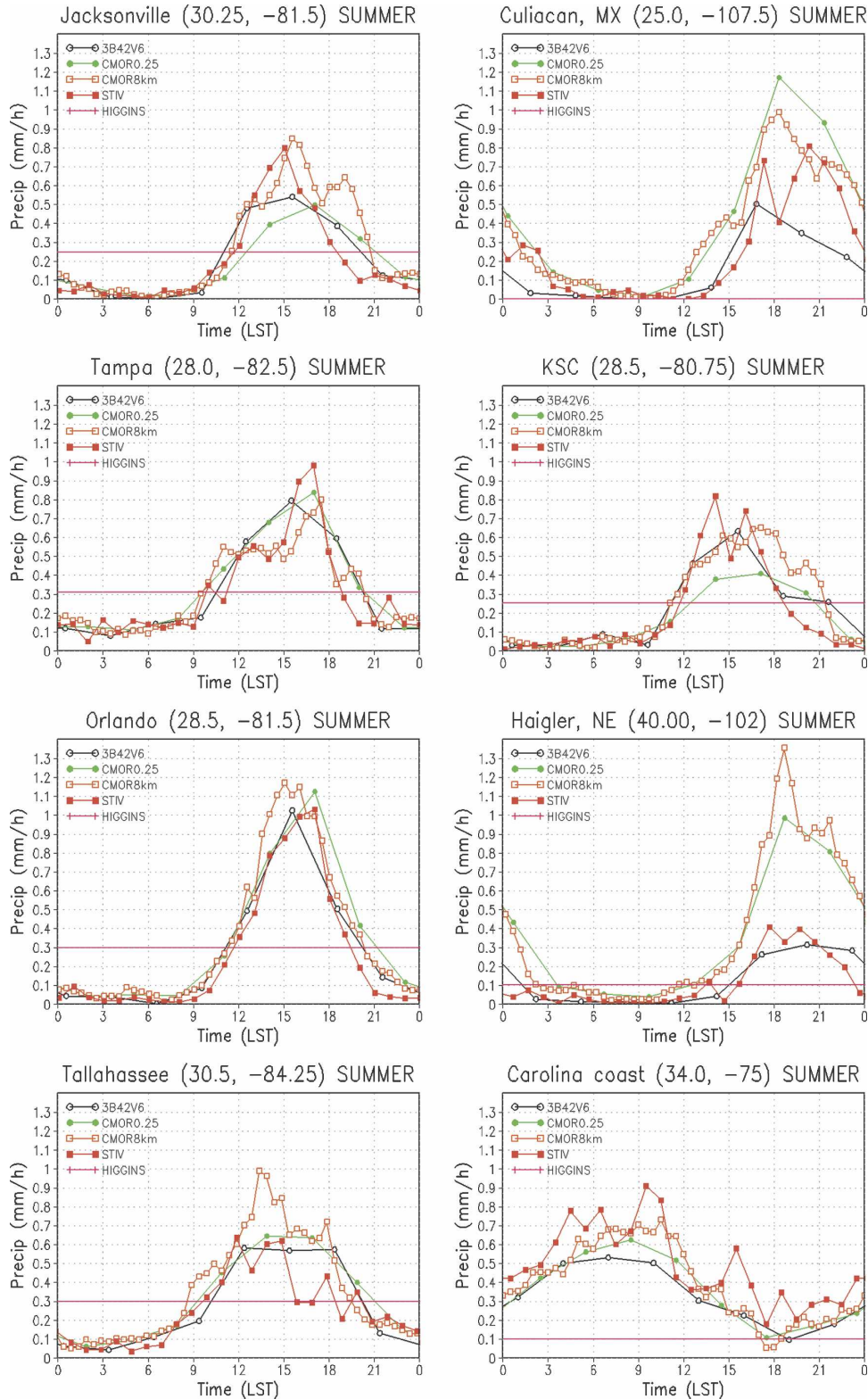
It is also noteworthy that CMORPH, which is based

Fig. 13. Climatology of daily precipitation time series at eight locations over CONUS (and the NAME region) in summer months (JJA). Five datasets are plotted: 3B42, CMOR0.25, CMOR8km, stage IV, and Higgins, at their respective native time resolutions. Higgins data are at daily resolution, so no diurnal variations can be shown, but are plotted here for comparison with the other datasets. There is no Higgins data coverage over Culiacan, Mexico.
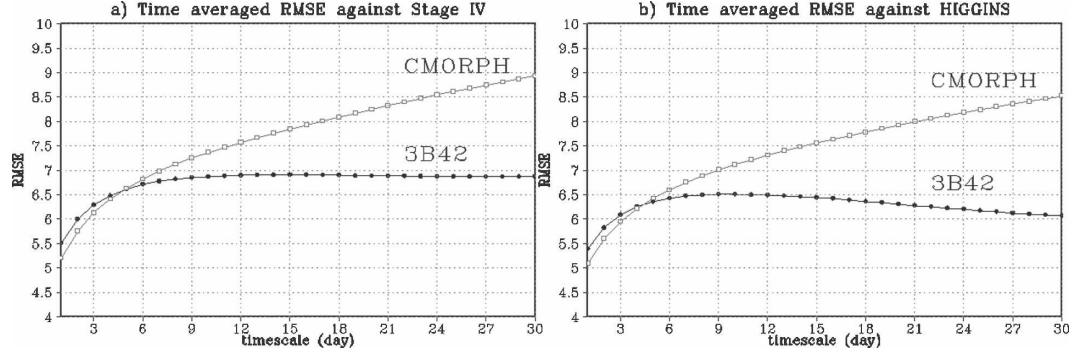
FIG. 14. Time-averaged RMSE for March 2003 through February 2006, for the satellite products (3B42 and CMORPH) compared with (a) stage IV and (b) Higgins, at time scales from 1 to 30 days. The RMSE values are rescaled by a factor of sqrt(N), where N is the time scale (number of days).

entirely on remote sensing data with no ground-based measurement information, did not perform significantly worse than 3B42. In some aspects, such as detection of rain events, CMORPH even outperformed 3B42. It remains to be seen how much the "morphing" technique employed in CMORPH helps with such improved detection performance. On the other hand, the relatively smooth propagation of precipitation events resulting from the "morphing" process might have missed the intermittent characteristics of precipitation, and it may contribute to the overestimates seen in summer. In addition, short-lived events such as thunder-

storms taking place between PMW scans will be missed by this procedure. Further studies and interactions with the data producers are needed to quantify these effects.

Based on our studies, we find the two TRMM-based datasets are very promising for land data assimilation applications, especially high-spatial-resolution studies such as those enabled by GSFC's Land Information System (LIS). We recommend using 3B42 for long-term, retrospective, and climatological studies due to its reduced biases on longer time scales, and CMORPH for short-term applications due to its higher probability of detection of rainfall events. However, special atten-
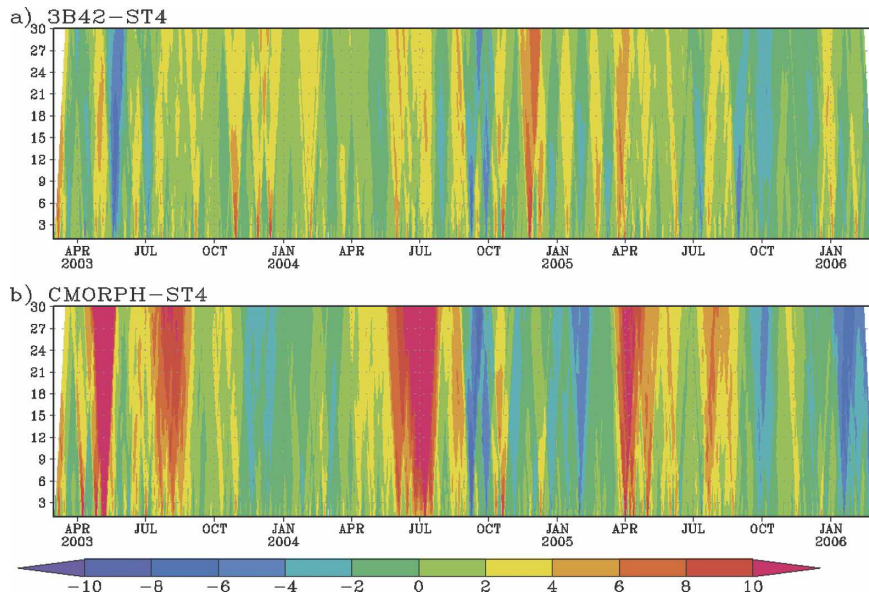

FIG. 15. Errors of area-averaged precipitation between the satellite products (3B42 and CMORPH) and stage IV over SE-US. The errors are computed at different time scales, after the precipitation data are averaged over each period from 1 to 30 days (ordinate). The errors are rescaled by a factor of sqrt(N), where N is number of days in the running average, to exaggerate the amplitude of the error at long time scales for display purposes.

tion needs to be paid when the differences in the satellite products can be possibly amplified, such as surface runoff studies and flood monitoring, due to the nonlinearity of these processes.

REFERENCES

Adler, R. F., P. R. Keehn, and I. M. Hakkainen, 1993: Estimation of monthly rainfall over Japan and surrounding waters from a combination of low-orbit microwave and geosynchronous IR data. *J. Appl. Meteor.,* **32,** 335–356.

——, C. Kidd, G. Petty, M. Morissey, and H. M. Goodman, 2001: Intercomparison of global precipitation products: The Third Precipitation Intercomparison Project (PIP-3). *Bull. Amer. Meteor. Soc.,* **82,** 1377–1396.

Briggs, P. R., and J. G. Cogley, 1996: Topographic bias in mesoscale precipitation networks. *J. Climate,* **9,** 205–218.

Dai, A., F. Giorgi, and K. E. Trenberth, 1999: Observed and model simulated diurnal cycles of precipitation over the United States. *J. Geophys. Res.,* **104,** 6377–6402.

Ebert, E. E., J. E. Janowiak, and C. Kidd, 2007: Comparison of near-real-time precipitation estimates from satellite observations and numerical models. *Bull. Amer. Meteor. Soc.,* **88,** 47–64.

Faures, J. M., D. C. Goodrich, D. A. Woolhiser, and S. Sorooshian, 1995: Impact of small-scale spatial variability on runoff modeling. *J. Hydrol.,* **173,** 309–326.

Fekete, B. M., C. J. Vorosmarty, J. O. Roads, and C. J. Willmott, 2003: Uncertainties in precipitation and their impact on runoff estimates. *J. Climate,* **17,** 294–304.

Ferraro, R. R., E. A. Smith, W. Berg, and G. J. Huffman, 1998: A screening methodology for passive microwave precipitation retrieval algorithms. *J. Atmos. Sci.,* **55,** 1583–1600.

Gottschalck, J., J. Meng, M. Rodell, and P. Houser, 2005: Analysis of multiple precipitation products and preliminary assessment of their impact on Global Land Data Assimilation System land surface states. *J. Hydrometeor.,* **6,** 573–598.

Grody, N. C., 1991: Classification of snow cover and precipitation using the Special Sensor Microwave Imager. *J. Geophys. Res.,* **96,** 7423–7435.

Gruber, A., X. Su, M. Kanamitsu, and J. Schemm, 2000: The comparison of two merged rain gauge–satellite precipitation datasets. *Bull. Amer. Meteor. Soc.,* **81,** 2631–2644.

Higgins, R. W., W. Shi, E. Yarosh, and R. Joyce, 2000: *Improved United States Precipitation Quality Control System and Analysis.* NCEP/Climate Prediction Center Atlas 7, 40 pp.

Hollinger, J., J. Pierce, and G. Poe, 1990: SSM/I instrument evaluation. *IEEE Trans. Geosci. Remote Sens.,* **28,** 781–790.

Hossain, F., and E. N. Anagnostou, 2004: Assessment of current passive-microwave- and infrared-based satellite precipitation remote sensing for flood prediction. *J. Geophys. Res.,* **109,** D07102, doi:10.1029/2003JD003986.

Huffman, G. J., and Coauthors, 1997: The Global Precipitation Climatology Project (GPCP) Combined Precipitation Dataset. *Bull. Amer. Meteor. Soc.,* **78,** 5–20.

——, R. F. Adler, M. Morrissey, D. T. Bolvin, S. Curtis, R. Joyce, B. McGavock, and J. Susskind, 2001: Global precipitation at one-degree daily resolution from multi-satellite observations. *J. Hydrometeor.,* **2,** 36–50.

——, and Coauthors, 2007: The TRMM Multisatellite Precipitation Analysis (TMPA): Quasi-global, multiyear, combined-sensor precipitation estimates at fine scales. *J. Hydrometeor.,* **8,** 38–55.

Imaoka, K., and R. W. Spencer, 2000: Diurnal variation of precipitation over the tropical oceans observed by TRMM/TMI combined with SSM/I. *J. Climate,* **13,** 4149–4158.

Janowiak, J. E., V. E. Kousky, and R. J. Joyce, 2005: Diurnal cycle of precipitation determined from the CMORPH high spatial and temporal resolution global precipitation analyses. *J. Geophys. Res.,* **110,** D23105, doi:10.1029/2005JD006156.

Joyce, R. J., J. E. Janowiak, P. A. Arkin, and P. Xie, 2004: CMORPH: A method that produces global precipitation estimates from passive microwave and infrared data at high spatial and temporal resolution. *J. Hydrometeor.,* **5,** 487–503.

Kummerow, A., and Coauthors, 2000: The status of the Tropical Rainfall Measuring Mission (TRMM) after two years in orbit. *J. Appl. Meteor.,* **39,** 1965–1982.

Lin, Y., and K. E. Mitchell, 2005: The NCEP stage II/IV hourly precipitation analyses: Development and applications. Preprints, *19th Conf. on Hydrology,* San Diego, CA, Amer. Meteor. Soc., 1.2.

Nijssen, B., and D. Lettenmaier, 2004: Effect of precipitation sampling error on simulated hydrological fluxes and states: Anticipating the Global Precipitation Measurement satellites. *J. Geophys. Res.,* **109,** D02103, doi:10.1029/2003JD003497.

Nykanen, D. K., E. Foufoula-Georgiou, and W. M. Lapenta, 2001: Impact of small-scale precipitation variability on larger-scale spatial organization of land–atmosphere fluxes. *J. Hydrometeor.,* **2,** 105–121.

Ogden, F. L., and P. Y. Julien, 1993: Runoff sensitivity to temporal and spatial precipitation variability at runoff plane and small basin scale. *Water Resour. Res.,* **29,** 2589–2597.

——, and P. Y. Julien, 1994: Runoff model sensitivity to radar precipitation resolution. *J. Hydrol.,* **158,** 1–18.

Rudolf, B., H. Hauschild, W. Rueth, and U. Schneider, 1994: Terrestrial precipitation analysis: Operational method and required density of point measurements. *Global Precipitation and Climate Change,* M. Desbois and F. Desalmond, Eds., NATO ASI Series I, Vol. 26, Springer-Verlag, 173–186.

Seo, D. J., 1998: Real-time estimation of precipitation fields using radar precipitation and rain gauge data. *J. Hydrol.,* **208,** 37–52.

Simpson, J., R. F. Adler, and G. R. North, 1988: A proposed Tropical Rainfall Measuring Mission (TRMM) satellite. *Bull. Amer. Meteor. Soc.,* **69,** 278–295.

Smith, E. A., and Coauthors, 2007: International Global Precipitation Measurement (GPM) program and mission: An overview. *Measuring Precipitation from Space: EURAINSAT and the Future,* V. Levizzani, P. Bauer, and F. J. Turk, Eds., Springer, 611–654.

Steiner, M., T. L. Bell, Y. Zhang, and E. F. Wood, 2003: Comparison of two methods for estimating the sampling-related uncertainty of satellite precipitation averages based on a large radar dataset. *J. Climate,* **16,** 3759–3778.

Vicente, G. A., R. A. Scofield, and W. P. Menzel, 1998: The operational GOES infrared rainfall estimation technique. *Bull. Amer. Meteor. Soc.,* **79,** 1883–1898.

Yang, S., and E. A. Smith, 2006: Mechanisms for diurnal variability of global tropical precipitation observed from TRMM. *J. Climate,* **19,** 5190–5226.